Automatic Dark Fibres Detection in Wool Tops

Juan Bazerque, Julio Ciambelli, Santiago Lafon, and Gregory Randall

Instituto de Ingeniería Eléctrica
Facultad de Ingeniería
Universidad de la República
randall@fing.edu.uy

Abstract. Is proposed a method for the automatic detection of dark fibres in wool tops based on image processing. A software which implements this method was developed, composed by five modules: KL projection, light correction, Gabor filtering, segmentation and morphology. The digital image are taken by a camera placed in a balanced illumination system. The method was calibrated and tested on 170 images marked by experts from Secretariado Uruguayo de la Lana.

Keywords: Dark Fibres Detection, Wool Industry, Balanced Illumination, Light Correction, Gabor Filtering

1 Introduction

1.1 Context

One of the problems of the wool industry is the presence of impurities in its raw material. One kind of this impurities are dark fibres coming from urine stain, black spots or other animal defects. These fibres remind coloured after the dying process, and appears as not desired dark lines, when tops destination is soft colour tissue production. Wool depreciates 15% [1] if it contains more than a specified number of dark fibres (DF) per Kg. The wool is collected from the sheep by shear, the fleece is then washed and combed. At this level the product is called wool top and is the input for the spinning industry.

In order to improve wool quality, is necessary to control the DF number as early as possible in the industrial process, but the difficulty of the problem is lower at the end of the industrial chain because the fibres are clean and parallelized. It exists a standardized method to manually count the DF per Kg on the top [2], in use at the Secretariado Uruguayo de la Lana (SUL).

In this article is presented an automatic solution for the counting module of DF in wool tops, integrating image processing techniques and the associated acquisition system.

1.2 Specification and Image Data Bases

Wool fibres are categorized by its coloration level in a 0 to 8 scale. The CSIRO standard [2] [3] defines as dark fibre those with level greater than 4 with the additional condition of being longer than $10mm$ [2].

A. Sanfeliu and J. Ruiz-Shulcloper (Eds.): CIARP 2003, LNCS 2905, pp. 367–374, 2003.

Fibres diameter are between 20 and 30μm. Working with a 1536x2048 resolution camera, a 18x24mm field of view was selected. A collection of 170 images of this size was acquired combining Merino and Corriedale races top samples. A SUL expert indicates the presence of DF in the images and gives its position and colour level. The data base formed by this images was divided in two groups, the A base, with 70 images for the system calibration and the B base reserved to validation. A new partition was made in de A base to form the sub-bases A1 and A2 with 20 and 50 images respectively.

1.3 Balanced Illumination System

To acquire the images the digital camera was placed on a controllable illumination system. The wool sample is placed between upper and below light sources. The light intensity is balanced to cancel white fibres shadows, vanish the background and enhance the presence of the DF [3][4]. Figure 1 shows the effect of this system comparing the same image acquired with wrong and balanced illumination.

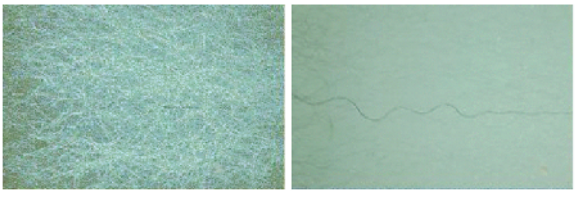

Fig. 1. Balanced illumination effect

2 Processes and Algorithms

2.1 Noise Reduction

The image is filtered by a median filter in order to reduce the image noise preserving borders [5].

2.2 Projection

The source image obtained from the balanced illumination system is RGB. To keep the software module compatible to a system implemented with an available high resolution B&W industrial camera, a projection was done at this point. In order to preserve as much DF information as possible in this process, a direction that statistically approximates the direction of the Karhunen Loeuve transform primary component was selected.

After finding this direction for the set of images in base A1, no relevant variation in its coordinates were found for other images. Therefore a statistically mean direction obtained in a training period was used to project the other images. This approximated direction was called AKL .

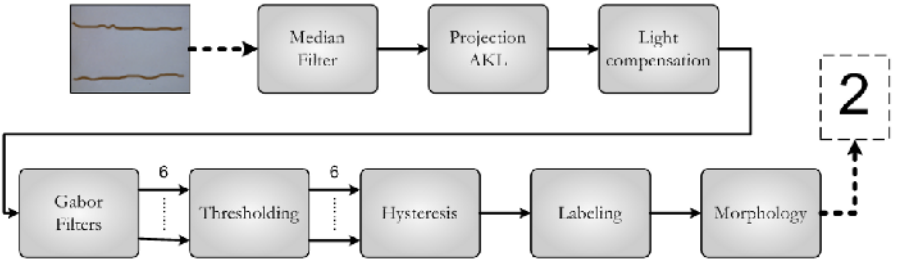

Fig. 2. Blocks diagram

2.3 Non Uniform Illumination Compensation

It was observed a non uniform illumination in the acquired images. The centre of the images are more illuminated than the border. Its effect is shown on figure 3 as athe surface representation.

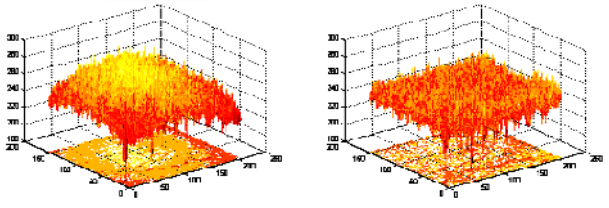

Fig. 3. Left: Surface representation of the acquired image. Rigth: image after non uniform illumination correction

To solve this problem a compensation step was introduced. A multiplicative model ($\mathcal{I}(x,y) = \mathcal{P}(x,y)\mathcal{F}(x,y)$) was supposed, where $\mathcal{I}$ is the original image, $\mathcal{F}$ represents the uniformly illuminated image and $\mathcal{P}$ is a parabolic surface with the maximum near the image centre. In order to estimate $\mathcal{P}$, a mean squares method is used with samples of $\mathcal{I}$ as input data. Knowing $\mathcal{I}$ and $\mathcal{P}$, is possible to correct the acquired image using the multiplicative model.

2.4 Gabor Filters

The aim of this process is to extract from the image as much information as possible about DF presence. Gabor Filters [6] are used in order to enhance the dark fibres in a textured white background. The bank of filters are tuned for a maximum response in presence of the outlying fibre depending on its direction and diameter.

Impulse response of this filters are deduced by scale transformation and rotations from the Gabor function (1) formed by a complex exponential modulated by a gaussian.

$$f(x,y) = \frac{1}{2\pi\sigma_x\sigma_y} e^{-\frac{1}{2}\left(\frac{x^2}{\sigma_x^2}+\frac{y^2}{\sigma_y^2}\right)} e^{2\pi j f_h x} \tag{1}$$

The basic frequency of the filters are represented by f_h. The impulse response of the Gabor filters are given by

$$f_{pq}(x,y) = \alpha^{-p} f(x^{'}, y^{'}) \tag{2}$$

$$x^{'} = \alpha^{-p}(xcos(\theta_q) + ysen(\theta_q)) \qquad y^{'} = \alpha^{-p}(-xsen(\theta_q) + ycos(\theta_q))$$

Where α^{-p} is the scale factor and θ_q the selected direction. Each filter acts as a directive bandpass filter with parameters p and q.

To design the filters, 3 central frequencies and 2 directions (vertical and horizontal) was chosen. The highest frequency was placed in $f_h = 1/8$. Following [7], with $S = 3$ and $L = 4$, were calculated the remaining filter parameters α, σ_x ,σ_y and the lower and medium frequencies f_l and f_m, getting the following parameters:

$$\alpha = 2 \qquad \sigma_x = 4.497 \qquad \sigma_y = 1.038 \qquad f_m = \frac{1}{16} \qquad f_l = \frac{1}{32}$$

To evaluate the filter orientations, the formule $\theta_q = \frac{\pi(q-1))}{L}$ was used, with $q = 1 \ldots 4$.

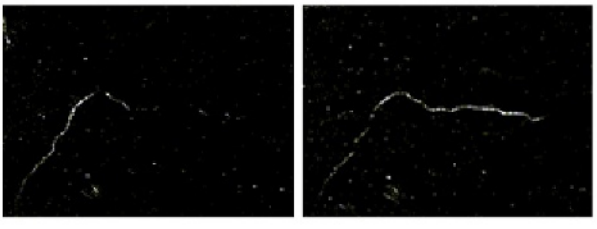

Fig. 4. Behaviour of two filters at the same frequency but in vertical and horizontal directions.

A FIR implementation was used for the filter realization. The used kernels are elongated, with axis size calculated in order to let place two times the Gaussian deviations in each direction.

The convolution kernel is applied to a subset of the input image formed by bidirectional subsampling in a 4 to 1 ratio.

Notice that the Gabor filtering separates the clusters corresponding to DF and background on the histogram of the image. Figure 5 shows the histogram of the expert marked pixels on the image before and after the Gabor filtering with an horizontal kernel.

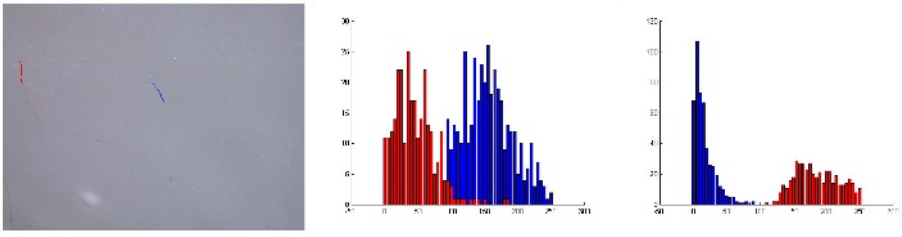

Fig. 5. Histogram of the expert marked pixels on the image before (left) and after (right) the Gabor filtering with an horizontal kernel.

2.5 Thresholding

The Gabor filter step generates 6 images: 2 orthogonal directions and 3 frequency bands. Each one is thresholded using a linear model in order to binarize the images after the Gabor filtering.

$$u_i = a_i\mu_i + b_i\sigma_i + c_i \quad i = 1 \ldots 6 \tag{3}$$

The parameters of the linear model are estimated in a learning process using the A1 image set. On this set an expert marked, for each Gabor filter response, a set of pixels corresponding to DF and another similar sized set for the background cluster. These sets carry the necessary information to estimate an optimal threshold for these responses, as explained in next section.

Parameters a, b and c of equation 3, are adjusted by a least squared method using the optimal thresholds estimated with the A1 data set.

Optimal threshold. Let be **J** a statistical error cost function formed by prior cluster probabilities $\mathcal{P}_F$ and $\mathcal{P}_B$ (DF and background respectively), the classification error probabilities α (classify a DF pixel as background) and β (classify a background pixel as DF), and the assigned error costs ($\mathcal{C}(\alpha)$ and $\mathcal{C}(\beta)$):

$$\mathbf{J} = \mathcal{P}_1\mathcal{C}(\alpha)\alpha + \mathcal{P}_2\mathcal{C}(\beta)\beta \tag{4}$$

The optimal threshold will be the minimum of **J** function. A Gaussian model for clusters distribution has been used.

The minimum of **J** function solves the next equation

$$(\sigma_F^2 - \sigma_B^2)x^2 + 2(\sigma_B^2\mu_F - \sigma_F^2\mu_B)x + \mu_B^2\sigma_F^2 - \mu_F^2\sigma_B^2 - 2(\sigma_F\sigma_B)^2 \ln(\lambda\frac{\sigma_F}{\sigma_B}) = 0 \tag{5}$$

$$\text{being} \quad \lambda = \frac{\mathcal{P}_B\mathcal{C}(\beta)}{\mathcal{P}_F\mathcal{C}(\alpha)}.$$

Once the Gaussian parameters μ_F, μ_B, σ_F and σ_B are extracted from the training test, optimal threshold is deduced from the equation 5. Changing the λ parameter allows the system to varies its sensibility, penalizing false positives or false negatives.

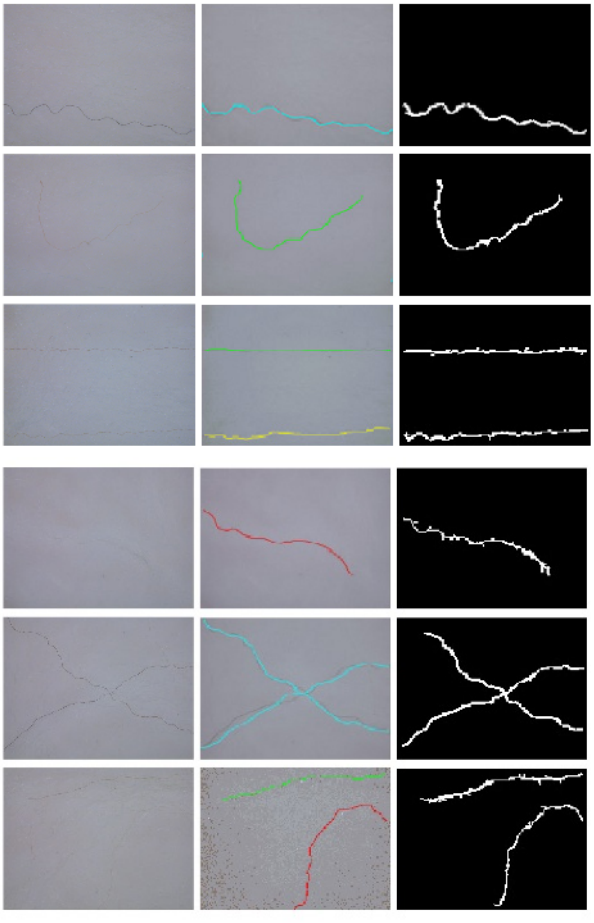

Fig. 6.

2.6 Dark Fibres Segmentation

Next step is to combine the 6 binarized images produced by the Gabor filter and threshold steps, into one bynary output image with DF pixels marked.

First, the 6 binarized images are added pixel a pixel. On that new image, a directive hysteresis was used in order to select the pixels belonging to DF.

Directional thresholding hysteresis is done using two thresholds T_{high} and T_{low}. Pixels with values surpassing the T_{high} are settled as DF starting points. A convenient direction is browsed for each starting point, and a walking process start adding pixels in this direction as the T_{low} test is passed.

At each step, the process allows direction to vary 30^o and if this test is not passed another intent is accomplished doubling the walking step.

Thresholds was settled to $T_{high} = 5$ and $T_{low} = [0.5, 3]$ according to the system sensitivity chosen.

2.7 Morphologic Operations

A labelling process [5] have been done on the resulting image, marking the regions which are associated to DF. The local and global angles, and the diameter are calculated for each region. This parameters are used to perform morphologic operations [13] to join regions belonging to the same dark fibres, and to eliminate small noisy regions.

3 Results

The image set B, formed by 100 images, were marked by an expert using the standardized manual procedure and processed by the automatic system. According to the SUL expert 87 of these 100 images has at least one DF. The total number of DF in the set is 118.

Table 1 presents the automatic success rates, categorized in fibres coloration levels, as the comparison between expert sentences and system sentences, applying to the same image. This table contains rates obtained placing $\lambda = 2$ and $T_{low} = 1.5$.

Table 1.

fibre kind	fibres detected by expert	system success	success rate	95% confidence interval
5	16	15	94%	(77%, 100%)
6	29	26	90%	(76%, 98%)
7	42	42	100%	(98%, 100%)
8	31	31	100%	(97%, 100%)

Added to the previous table, the system made two false negatives in the 100 images set.

Figure 6 illustrates some results. The first column shows the image after the non uniform illumination step. For each image, the second column shows the DF marked by the expert. The DF colour category is detailed in a colour scale as follows: red: 5, yellow: 6, green: 7 and cyan: 8. The third column shows the dark fibres detected by the automatic system.

References

1. Kremer, R.: *Personal communication* Facultad de Veterinaria, Universidad de la República.
2. Foulds, R.A., Wong, P., Andrews, M.W.: *Dark fibres and their economic importance* Wool technology and Sheep Breeding, Vol XXXII, N^o11, 91–100

3. *Wool Contamination: Detection of dark fibre contamination on Merino wool* Fact_sheet_018, July 2001. Queensland Department of Primary Industries; Queensland, Australia.
4. IWTO(E)-13-88 *Counting of Coloured Fibres in Tops by the Balanced Illumination Method*. International Wool Textile Organization, London, U.K.
5. González, R.C., Woods, R.E.: *Tratamiento Digital de Imágenes*. Addison-Wesley, 1992.
6. Mallat, S.: *A Wavelet Tour of Signal Processing*, Academic Press, 1998
7. Kumar, A., Pang,G.K.H.: *Defect Detection in Textured Materials Using Gabor Filters*, IEEE Transactions on Industry Applications Vol 38, N^o.2, March/April 2002.
8. Kittler, J.; *Pattern Recognition*, University of Surrey, Spring semester 1999.
9. DeHoff, R.: *The Essential Guide to Digital Video Capture*, Imagenation Corporation.
10. West, P.: *A Roadmap for Building a Machine Vision System*, Automated Vision Systems, Inc.
11. Delfosse, P., Galère, H., Grignet, J., Lemaire, P., Lkèonard, J., Longrèe, M., Muller, J., Paquet, V.:*Maesurement of Cleanliness in Combed Wool by Artificial Vision and Image Processing* The 9^{th} International Wool Textile Reserch Conference, Vol 4, 97–105, June/July 1995.
12. Russ, J.C.: *The Image Processing Handbook* CRC Press Second Edition, 1994.
13. Coster, M.,Chermant, J.L.: *Precis d'Analyse d'Images* Presses Du CNRS, 1989.